On the hydration of ternesite and the formation of thaumasite

I. Galan [a],[*], F.R. Steindl [a],[b], C. Grengg [a], M. Dietzel [a], F. Mittermayr [b]

[a] *Institute of Applied Geosciences, Graz University of Technology, Graz, Austria*
[b] *Institute of Technology and Testing of Construction Materials, Graz University of Technology, Graz, Austria*

ARTICLE INFO

ABSTRACT

The calcium sulfosilicate phase ternesite, previously considered as an undesired product in cement kilns, has recently gained attention due to its potential replacement of ye'elimite in calcium sulfoaluminate clinkers and the contribution of ternesite hydration products to the strength development of such clinkers. However, the potential formation of thaumasite during ternesite hydration, in particular in the presence of ettringite, has not yet been fully explored. In the present study synthesized ternesite was hydrated in the presence of ettringite, carbonated ettringite, portlandite and calcite. Thaumasite formed, together with gypsum and C-S-H, only in samples initially containing ettringite, both at 6.5 °C and at ambient temperature. Portlandite and calcite did not have a noticeable impact on the hydration of ternesite and the formation of thaumasite. The dissolution and/or carbonation of ettringite, together with its surface template effect, is suggested to be key to initiate thaumasite nucleation via the solid solution route.

1. Introduction

Calcium sulfosilicate clinkers have attracted attention in the past years since the hydraulic behaviour of the main phase, ternesite (5CaO·2SiO₂·SO₃), was verified [1–3]. The presence of this phase in calcium sulfoaluminate (CSA) systems and thus, the partial substitution of ye'elimite (4CaO·3Al₂O₃·SO₃), helps lowering the need of alumina in the raw materials, one of the main drawbacks of CSA cements [4,5]. However, before this type of clinkers can be implemented, durability issues such as the potential formation of thaumasite during the hydration of ternesite or upon exposure of the hardened material to the environment need to be assessed.

Although the 'thaumasite form of sulfate attack' on concrete and its disastrous consequences have long been known, formation conditions and stability of thaumasite (CaO·SiO₂·CaCO₃·CaSO₄·15H₂O), are still under discussion. Most theories proposed to explain thaumasite formation envisage the presence of ettringite (3CaO·Al₂O₃·3CaSO₄·32H₂O) acting either as a precursor to thaumasite in the so-called woodfordite route [6–8] or as providing functional surface groups for heterogeneous thaumasite nucleation [9]. Another pathway for thaumasite formation, the so-called direct route, does not involve the presence of ettringite, and formation takes place by reaction of C-S-H with carbonate, sulfate, calcium ions and excess water [7]. Kinetics of nucleation and growth of thaumasite in cement systems are often slow: the rather limited

availability of silicic acid in cement pore fluids and the comparable fast precipitation rates of potentially competing phases (e.g. ettringite, gypsum, calcite) causes thaumasite to mostly form over time periods of several years in real technical settings. In most cases formation of thaumasite is reported at temperatures below 15 °C [10,11], where calcium carbonate solubility is enhanced and higher coordination degrees of Si in respect to the oxygen of H₂O are favored [12].

Limestone filler in the cement, limestone aggregates (or the corresponding hydration products, e.g. CO₃-AFm) and groundwater are common sources to provide carbonate ions to form thaumasite [6,13,14]. Atmospheric CO₂ can also act as a source for aqueous carbonate ions [15], in particular by considering the high absorption rates of gaseous CO₂ into strongly alkaline solutions, e.g. [16]. Many cases of thaumasite formation are reported below grade, which may again be related to groundwater bicarbonate originated from CO₂ of soils and/or limestone dissolution. In addition to the main ingredients needed for the formation of thaumasite, organics such as sucrose and other cement-hydration controlling admixtures have been proven to promote and accelerate thaumasite formation [12,17,18].

While noticeable thaumasite formation in real structures usually occurs over long time periods, e.g. [6,19,20], Dvorak and co-workers have recently reported rapid formation of thaumasite during the hydration of calcium sulfosilicate clinkers stored at 5 °C [21,22]. Ska-lamprinos et al. pointed to the rapid formation of a thaumasite-like

---

phase during the hydration of pure ternesite [2]. The authors claimed that the applied hydration stopping method with acetone may have promoted the formation of this phase as a result of a secondary reaction between C-S-H, gypsum and carbon dioxide in the presence of the solvent. In this case, however, formation of ettringite from Al impurities present in the raw materials cannot be ruled out. Such small amounts, <4 %, make the absolute differentiation between ettringite and thaumasite via XRD difficult. In suspensions prepared with clinkers containing ternesite, belite, anhydrite and lime, formation of 10–20 % thaumasite was reported in the hydrated pastes after 180 days [21], which was attributed to the reaction of gypsum (from the hydration of anhydrite and ternesite), silica and carbon dioxide.

The presence of alumina in ternesite systems has been shown to activate ternesite hydration, yielding different hydration products like C-S-H, straetlingite, katoite, ettringite or AFm, depending on the alumina source (Al(OH)$_3$, CSA or calcium aluminates) [23–27]. However, the reactions taking place in complex systems containing ternesite have not been fully assessed. In the present study the focus was placed on simplified systems and the fundamental understanding of ternesite hydration in the presence/absence of various additions. As ettringite is in many reported cases the trigger for thaumasite formation and because ettringite forms readily in CSA clinkers before ternesite starts to hydrate, ternesite was hydrated in the presence of ettringite. Additionally, the possible effect of calcite and portlandite in the hydration process, as well as the impact of particle size and temperature, are reported.

2. Materials, experiments and methods

2.1. Materials

The ternesite samples used had been previously synthesized by mixing stoichiometric amounts of belite and calcium sulfate, with additional 0.2 wt% K$_2$O, 0.1 wt% Na$_2$O and 0.4 wt% MgO. The previously synthesized belite, obtained by clinkering stoichiometric amounts of SiO$_2$ and CaCO$_3$ at 1300 °C for 3 days, consisted of 62 ± 5 wt% γ-belite and 38 ± 5 wt% of β-belite. The mixes of belite and calcium sulfate were heated at 1175 °C and left reacting for 1 day, as described in [2].

The purity of ternesite was ~94 wt% as determined by XRD plus Rietveld refinement; other phases present were β-belite ~4 wt%, γ-belite ~2 wt%, and anhydrite <0.5 wt%. The obtained product was ground in a micronising mill (McCrone) with agate grinding elements and ethanol in 5 gram batches in 10 minute cycles. After 2 and 7 grinding cycles BET values of 3.5 and 8.4 m^2/g respectively, were reached. The ternesite samples obtained from the 2 grinding processes were called T$_{3.5}$ (BET 3.5 m^2/g) and T$_{8.4}$ (BET 8.4 m^2/g).

Ettringite, carbonated ettringite, portlandite and fine calcite were added to the ternesite samples to assess their effect during hydration. Ettringite was synthesized according to Balonis et al. [28] with a purity > 99 % (BET surface area 10.1 m^2/g). The carbonated ettringite was produced by storing synthesized and ground ettringite in low density PE containers at room temperature for 1 year. The crystalline composition of the carbonated ettringite was: 72 wt% ettringite, 10 wt% calcite, 11 wt% gypsum and 7 wt% basanite (see Fig. A1 in the Appendix) and the BET surface area was ~15 m^2/g (note the carbonated ettringite partially

decomposed during the BET measurement). Commercial powders of calcium hydroxide (Merck, Germany, purity > 99 %, BET surface area 15.2 m^2/g) and fine limestone (Betocarb UF, Omya, Austria, d$_{50}$: 0.9 μm; BET surface area 8.2 m^2/g) were used.

2.2. Experiments

T$_{8.4}$ and T$_{3.5}$ samples were mixed with distinct amounts of ettringite, portlandite, carbonated ettringite and fine calcite (see Table 1). The additions were chosen according to their potential to modify the hydration process of ternesite and to promote thaumasite formation. To reach the potentially most favorable conditions for thaumasite formation, samples with the highest BET surface area, T$_{8.4}$, were mixed with carbonated ettringite containing both ettringite and calcite. Additionally, portlandite was added to T$_{8.4}$ to assess the potential acceleration of thaumasite formation as a result of the high pH buffering, as reported by [21]. To deconvolute the effects of ettringite and calcite, samples with lower BET surface area were mixed with ettringite, carbonated ettringite and calcite. Portlandite was skipped for these samples after proving it had almost no effect on T$_{8.4}$ hydration.

Samples containing T$_{8.4}$ and T$_{3.5}$ were named T1 and T2, respectively. Additionally, in samples containing calcite, portlandite, ettringite or carbonated ettringite the letters C, P, E and CE, respectively, were added to T1 or T2. Samples containing T$_{8.4}$ and T$_{3.5}$ were hydrated using a water:solid ratio of 1 and 0.7, respectively. After 2 minute hand mixing the samples were poured in round sample holders with a diameter of 32 mm and a height of 3 mm.

The hydrated samples containing T$_{8.4}$ (T1) were exposed at room temperature and at 6.5 ± 0.3 °C for up to 4.5 months. The hydrated samples containing T$_{3.5}$ (T2) were exposed at room temperature (22 ± 3 °C) for 1.3 years. In all cases 'humid curing' (RH 95–99 %) conditions were applied: the samples were placed in closed containers with water (where the samples did not touch the water). The containers were periodically opened allowing for the renewal of the inner atmosphere. The cold storage conditions were chosen to assess the potential enhancement/acceleration of thaumasite formation at low temperature as compared to room temperature conditions. Similarly, high humidity was selected to prevent any hydration restrictions and to allow for the potential formation of thaumasite.

2.3. Methods

The following characterization methods were applied: X-ray diffraction (XRD), BET specific surface area determination, Scanning Electron Microscopy (SEM) and Electron Probe Microanalysis (EPMA). The XRD equipment was a PANalytical X'Pert PRO diffractometer, fitted with a Co X-ray tube operated at 40 kV and 40 mA. Surface and bulk measurements were carried out. Surfaces were directly scanned by placing the whole sample in a sample holder. For the bulk measurement pieces were taken and homogeneously ground. Rietveld refinement was carried out with Highscore Plus (see Table A1 for the crystal structures used). Multi-point BET analyses were performed on a BELSORP-miniX at 77 K using N$_2$ as adsorptive gas. SEM images of gold coated samples were obtained with a Carl Zeiss DSM 982 Gemini microscope fitted with a thermal field emission gun at an acceleration voltage of 5 kV. For

Table 1
Composition of powder samples prepared for the experiments (in mass percent) and storage conditions.

Samples	Ternesite T$_{8.4}$	Ternesite T$_{3.5}$	Ettringite	Carbonated ettringite	Fine calcite	Portlandite	Temperature
T1	100						6.5 °C & room T
T1-CE	95			5			6.5 °C & room T
T1-P	90					10	6.5 °C & room T
T2		100					Room T
T2-E		95	5				Room T
T2-CE		95		5			Room T
T2-C		95			5		Room T

EPMA analyses, samples were embedded in epoxy resin. Cross sections were cut using a diamond saw, polished and carbon coated. The samples were then analyzed with a JEOL JXA8530F Plus Hyper Probe. Semi-quantitative elemental distribution maps of calcium, silicon, sulfur and aluminium were obtained in the wavelength-dispersive mode with an acceleration voltage of 15 kV, a beam current of 10/20 nA, a dwell time of 12/20 ms and a pixel size of 1/3 μm. Elemental mappings were quantified against the following certified mineral standards: augite for Ca, microcline for Al and Si, and barite for S. The obtained elemental mappings were further processed with XMapTools 4 beta 2 [29] to produce space-resolved phase distribution mappings.

A schematic experimental work-flow is shown in Fig. 1.

3. Results and discussion

3.1. T1 samples with higher surface area stored at 6.5 °C and room temperature

After 2 months exposure at 6.5 °C the expected ternesite hydration products, C-S-H and gypsum, had formed in all 3 $T_{8.4}$-containing samples (T1, T1-CE and T1-P), according to XRD analyses (Fig. 2). Additionally, on the surface of T1 samples stored at 6.5 °C calcite and monohydrocalcite had formed (Fig. 2). Anhydrous ternesite was also detected in all cases (see Table A2). Negligible differences were observed between samples with portlandite (T1-P) and without (T1). However, important differences were noticed in samples with initial carbonated ettringite (T1-CE). Considerable amounts of thaumasite formed in T1-CE after 2 months, whereas in T1 and T1-P only traces of thaumasite were identified (Fig. 2). From 2 to 4.5 months little mineralogical changes were observed on the surface and in the bulk: thaumasite increased slightly in T1-CE and gypsum decreased. Formation of thaumasite was clearly demonstrated based on 2 evidences: (i) the unit cell parameters of the phase formed in T1-CE clearly agree with those of thaumasite [30,31] (see Table A3 in the Appendix), and (ii) the amount of phase formed, with respect to the initial amount of ettringite (see initial XRD patterns in Fig. A2), would not have been possible for ettringite due to the lack of aluminium in the system.

In samples stored at room temperature a similar bulk behaviour was observed after 2 months: thaumasite only formed in samples that had been initially intermixed with 5 % of carbonated ettringite. Higher temperatures did not prevent formation of thaumasite in T1-CE, in fact larger amounts of thaumasite (with respect to the total crystalline phases) formed in the sample exposed at room temperature than in that at 6.5 °C. This fact correlates with the hydration degree which was considerably higher in T1-CE stored at room temperature. Most importantly, the sample T1-CE stored at room temperature started showing physical expansion and structural disintegration after 2 months. No changes in appearance were visually observed in sample T1-CE after 2 months at 6.5 °C.

The morphology of the calcium carbonates formed on the surface of the samples stored at 6.5 °C for 4.5 months, as observed by SEM, consisted of monohydrocalcite, partially destroyed and dehydrated probably due to the exposure to higher temperatures and high vacuum during analyses (Fig. 3a). The calcite formed on the surface of T1 samples at 6.5 °C showed scalenohedral shape (Fig. 3b), which is expected at high growth rates in the presence of sulfate [32]. The microstructure of T1-CE bulk was not homogenous, mainly 3 different regions can be
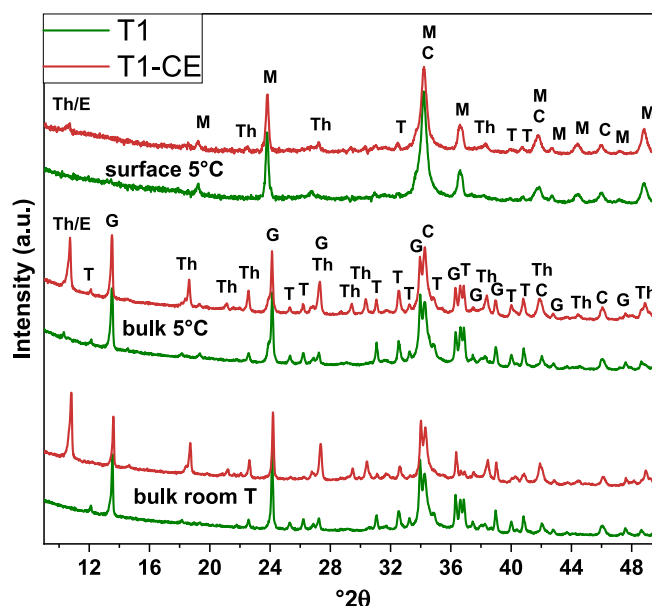

Fig. 2. XRD patterns of hydrated ternesite samples T1 and T1-CE after 2 months exposure at 6.5 °C and room temperature. Th: thaumasite. E: ettringite, M: monohydrocalcite, G: gypsum, C: calcite, T: ternesite. Note for simplicity only the first peak is marked with Th/E; in the rest of the reflections marked with Th a small contribution of ettringite is included.

distinguished: (i) intermixed C-S-H and gypsum crystals with some thaumasite needles (Fig. 3c), (ii) areas with thaumasite (Fig. 3d) and (iii) regions with mostly gypsum and minor thaumasite (Fig. 3e). The microstructure of T1 and T1-P consisted mostly of C-S-H intermixed with crystals of gypsum (Fig. 3f).

3.2. T2 samples with lower surface area stored at room temperature

After 1.3 years C-S-H and gypsum had formed in all 4 $T_{3.5}$-containing samples (T2, T2-C, T2-CE and T2-E), according to XRD analyses and SEM observations (Figs. 4, 5a and b). Additionally, calcite and aragonite were also detected in all cases (Fig. 4). Ternesite was present in all samples except in the one with ettringite T2-E, where both the hydration and the carbonation degree were considerably higher (see Table A4). Negligible differences were observed between the sample containing fine calcite, T2-C, and the one without additions, T2. Thaumasite had formed in samples containing initial ettringite, T2-E and T2-CE: the higher the initial ettringite content, the more thaumasite had formed (Fig. 4). According to the Rietveld refinement, thaumasite constituted ∼25 % of the total crystalline phases in T2-E, whereas ettringite was <5 % (Table A4). In T2-CE, where formation of thaumasite was less developed, the distinction between the above two phases is not so clear. Substitution of up to 50 % Al by Si in ettringite and of up to 3 % Si by Al in thaumasite is expected within the thaumasite-ettringite solid solution series [33,34] which means the Al—Si replacement is restricted, especially in the case of thaumasite.

The particle size of the samples played a major role in the hydration reactions. Increasing the specific surface area from 3.5 to 8.4 m^2/g led to an acceleration in the formation of C-S-H and gypsum in all cases, and of thaumasite in the samples with initial ettringite. Lower amounts of ternesite (in crystalline wt%) were found in T1 samples after 2 months compared to T2 samples after 1.3 years (∼35 % versus ∼50 % in samples without ettringite).

The microstructure of T2 samples consisted of intermixed C-S-H and gypsum (Fig. 5a). In samples with initial ettringite, additional thaumasite needles were observed within the matrix (Fig. 5b). In terms of physical stability, none of the samples showed signs of expansion or
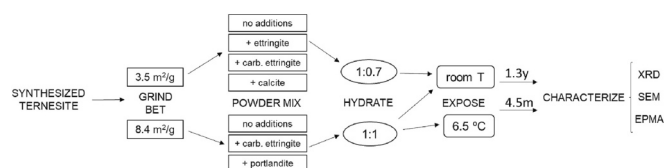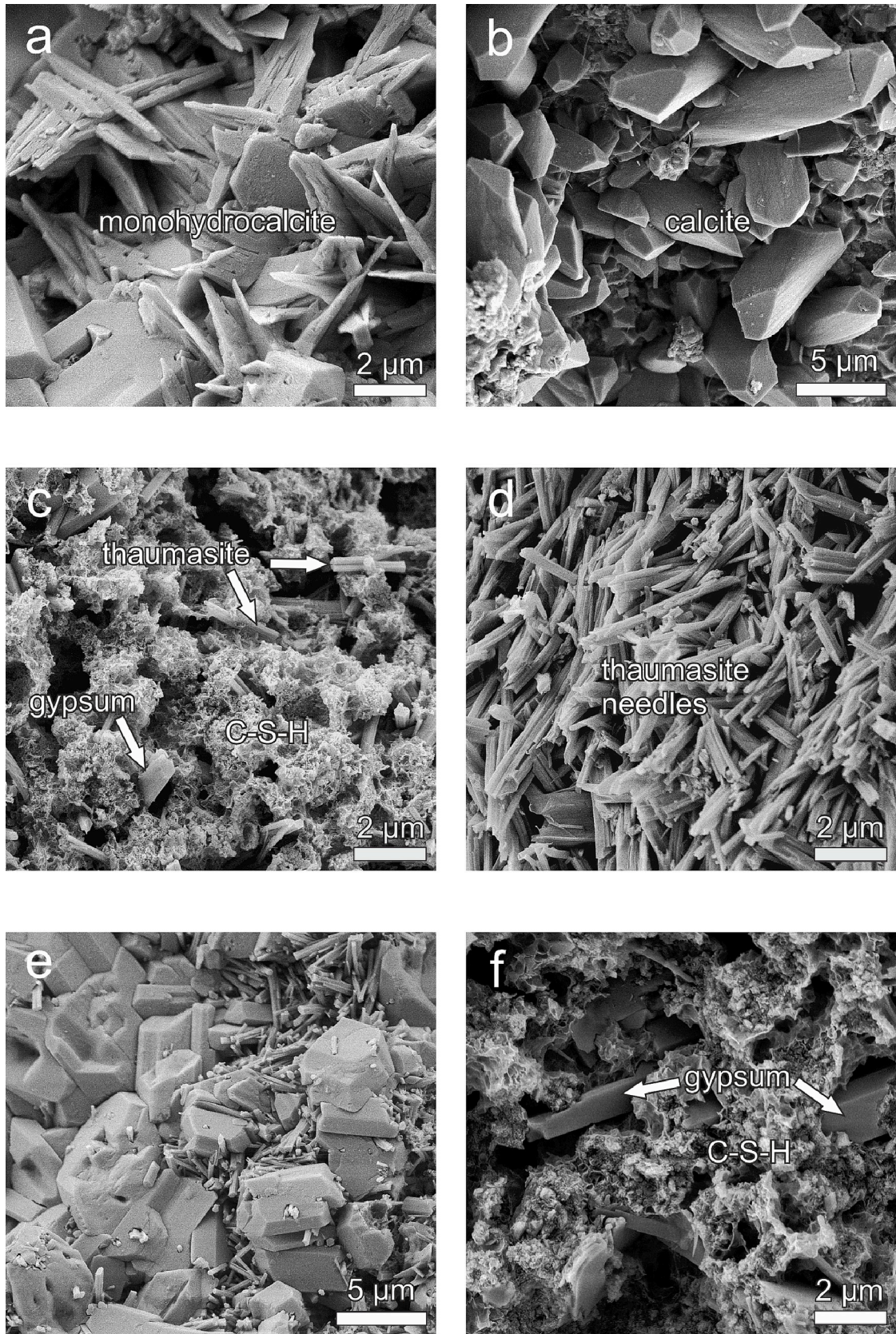

Fig. 1. Experimental work-flow scheme.

Fig. 3. SEM images of samples stored at 6.5 °C for 4.5 months: surface of T1-CE (a), surface of T1 (b), bulk of T1-CE (c, d, e), bulk of T1 (f).
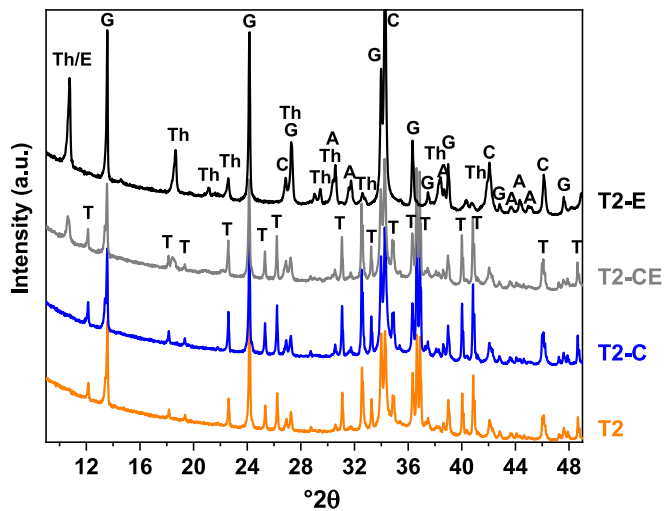
Fig. 4. XRD patterns of hydrated T2 samples (without additions T2, with calcite T2-C, with carbonated ettringite T2-CE and with ettringite T2-E) after 1.3 years exposed at room temperature. Th: thaumasite. E: ettringite, G: gypsum, C: calcite, A: aragonite, T: ternesite. Note for simplicity only the first peak is marked with Th/E; in the rest of the reflections marked with Th a small contribution of ettringite is included.

disintegration; the only feature visually observed in sample T2-E was the lighter color of the layer formed on the surface as a result of carbonation.

EPMA elemental mappings revealed the distribution of gypsum within the T2 matrix (Figs. 6a and A3). Gypsum-rich regions, indicated by the higher S content (and lower Si), were not only found intermixed with the C-S-H in the matrix but also on the rims of partially dissolved/hydrated ternesite grains. Apart from the carbonation layer on the surface of the sample (indicated by the high Ca, low Si and almost no S), sample T2 presented a homogenous matrix. In the partially hydrated ternesite grains, distributed all over the matrix, the lower S content, compared to the stoichiometric S content in ternesite, points to a partial and incongruent dissolution/reaction. Hydration of ternesite seems to have started by the dissolution of the sulfate followed by calcium and finally the silicate which seems to be the least mobile. This kinetically driven incongruent reaction process could also explain the accumulation of gypsum in certain regions within the matrix.

In the samples with initial ettringite, T2-CE and T2-E, formation of

thaumasite was directly linked with the presence of Al, and thus spatially with the initial ettringite. Rounded areas with an ettringite-rich core (higher in S and Al) and a thaumasite-rich rim (higher in Si) were observed all over the matrix (Figs. 6 and A4). The differences in composition of the ettringite-thaumasite features could be clearly resolved for the bigger 'grains' (Fig. 7): the inner core, with ettringite and gypsum, transforms progressively into thaumasite, with a gradual decrease of Al (and S) concentration. Plotting the molar ratios of Al/Si of the highlighted area across an ettringite-gypsum-thaumasite grain (see Fig. 7) revealed that in the transition from ettringite to thaumasite a woodfordite-like composition with a ratio of 1 had formed. Thereafter a step drop in Al/Si ratio suggests formation of pure thaumasite (see also [33,34]).

The sample with initial ettringite, T2-E, showed a very loose surface with formations of calcium carbonate, gypsum, and cracks/voids, followed by a very compact carbonation layer (Figs. 6b and A4). The matrix below the carbonation layer indicated a significant decalcification and Si-enrichment. Together with the ettringite-thaumasite features, gypsum-rich areas as well as thin long veins of gypsum/thaumasite formed in the matrix, typically connecting the ettringite-thaumasite-regions.

The presence of carbonated ettringite, with minor contents of gypsum, calcite and bassanite, did not seem to accelerate the process of thaumasite formation when compared to the presence of uncarbonated ettringite. The sulfate needed could already be provided by the gypsum formed during hydration and as such the extra calcite and bassanite provided by the carbonated ettringite did not seem to be needed. In fact, the partial carbonation of ettringite seemed to slightly reduce thaumasite formation. The presence of calcite, in sample T2-C, was not decisive for providing aqueous carbonate ions because (i) the solubility of calcite is very low under the prevailing alkaline conditions and (ii) aqueous carbonate is provided at a high level via the absorption of atmospheric CO_2.

4. Summary and implications for ternesite-based cements

Despite the availability of all ingredients needed for its formation, thaumasite did not form during the hydration of pure ternesite, neither at low nor at room temperature, in the time frames considered (1.3 years for the lower and 4.5 months for the higher specific surface area ternesite).
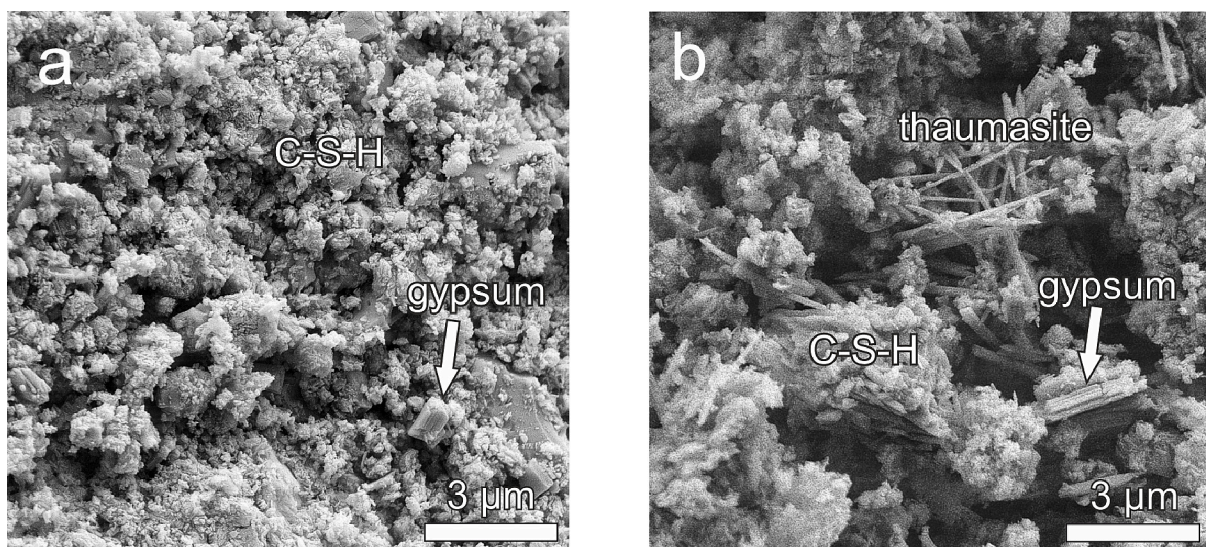

Fig. 5. Micrographs of T2 (a) and T2-E (b) after 1.3 years exposure at room temperature.
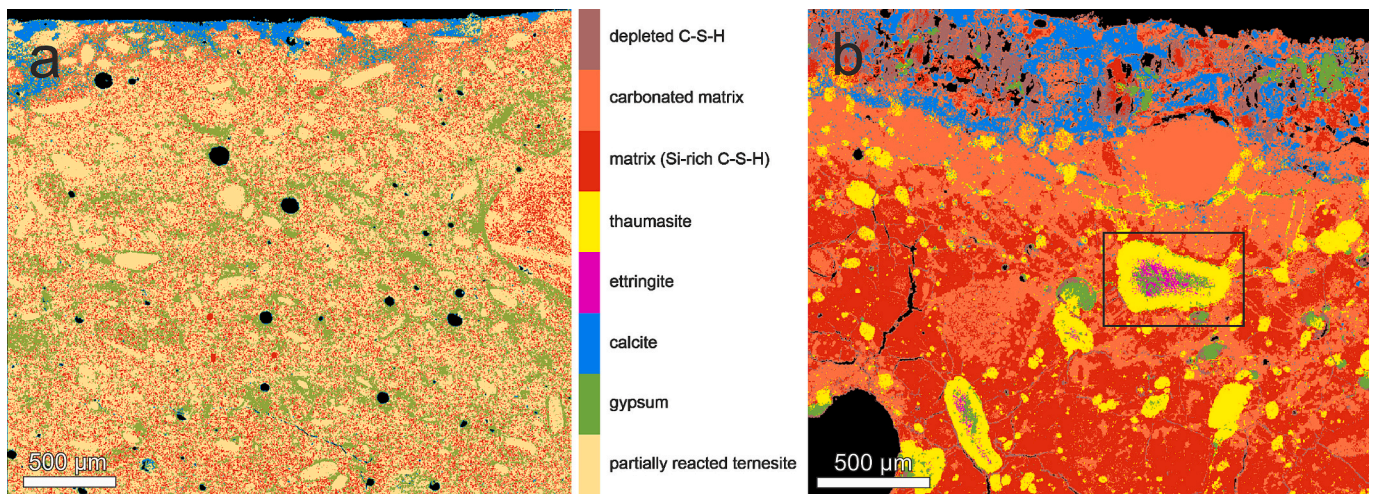
Fig. 6. EPMA phase mappings of samples T2 (a) and T2-E (b) after 1.3 years exposure at room temperature. For detailed elemental mappings of the samples see Figs. A3 and A4. The black rectangle in T2-E marks a region of varying ettringite/thaumasite composition.
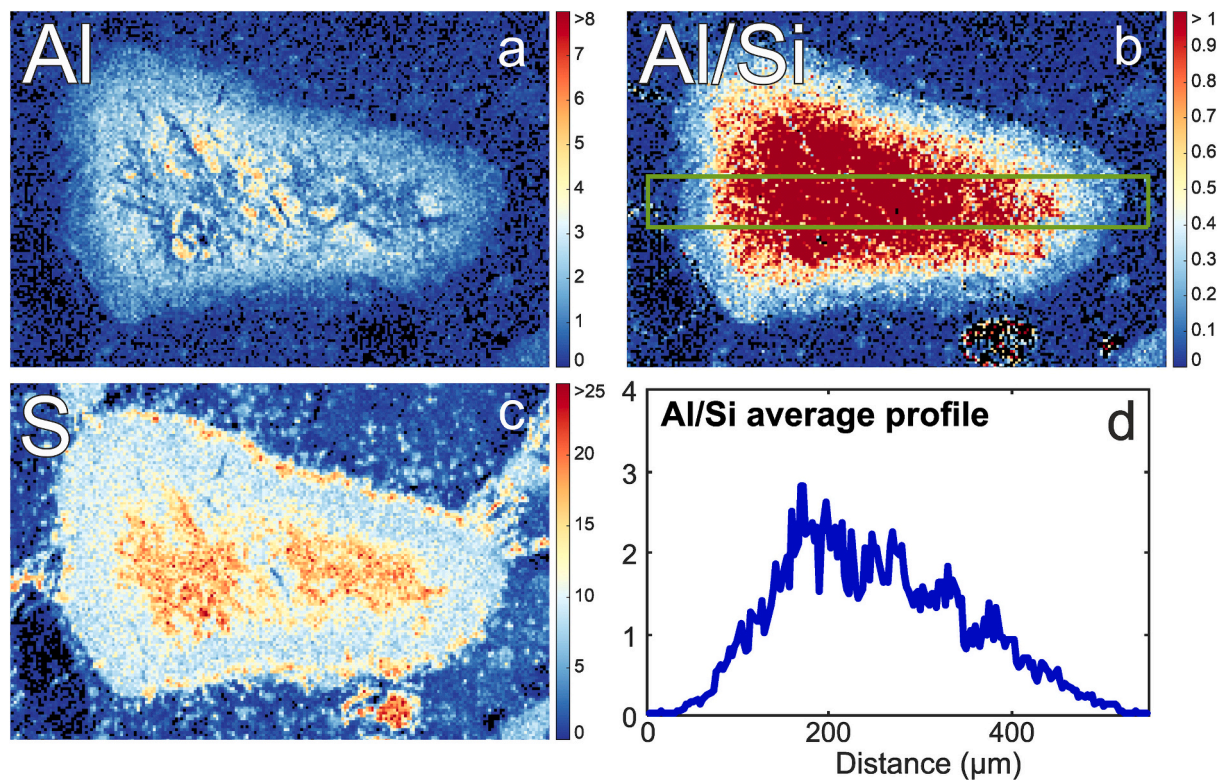

Fig. 7. Al and S elemental mappings (% mass) of an ettringite-thaumasite 'grain' (marked by black rectangle in Fig. 6) in sample T2-E after 1.3 years exposed at room temperature (a). Map and profile of Al/Si molar ratio. The green bar marks the region sampled for generating the Al/Si profile shown below (b). (For interpretation of the references to color in this figure legend, the reader is referred to the web version of this article.)

4.1. Presence of portlandite and calcite

The presence of portlandite and calcite in the systems did not promote the formation of thaumasite. This is in contrast to Dvorak et al., who reported portlandite to favor thaumasite formation as preserving strongly elevated pH [21]. From field studies however, it is also known that the bulk formation of thaumasite takes place at pH lower than 12 [35]. In cement chemistry it is accepted that the presence of portlandite is detrimental when concrete is exposed to sulfate attack because (i) it provides Ca^{2+} for the formation of gypsum, ettringite and thaumasite, (ii) it conditions the chemical composition of the C-S-H and (iii) it forms

preferentially in the ITZ around the aggregates and has therefore a negative effect on the aqueous diffusion of sulfate ions. According to Bellmann et al. the presence of portlandite is accompanied by high molar Ca/Si ratios of C-S-H (in the range 1.6–1.8), which converts easier to thaumasite (when the rest of the conditions are met) than silicon-rich C-S-H (Ca/Si 0.8–1.2), which shows higher resistance against the thaumasite form of sulfate attack [36]. In the present study, the Ca/Si molar ratio of C-S-H formed by ternesite hydration is estimated at 2.2 ± 0.3 (T2 sample). No portlandite was detected either by XRD or EPMA in the present study, in agreement with [2]. Although the exact stoichiometry of the reaction is not known, a general hydration equation can be

assumed:

$$5CaO \cdot 2SiO_2 \cdot SO_3 + nH_2O \rightarrow$$
$$(3 + x)CaO \cdot 2SiO_2 \cdot mH_2O + (1 - x)Ca(OH)_2 + CaSO_4 \cdot 2H_2O$$
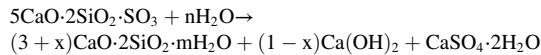
In the systems studied, the addition of extra portlandite does not seem to contribute to the susceptibility of the system towards thaumasite formation as the pH value and the Ca/Si ratio are probably already in the optimal range for its development.

Similarly, the presence of fine calcite did not show any effect and no hydration products containing carbonate were detected. In the samples where thaumasite formed the carbonate needed was obtained from the atmosphere. Calcite solubility is very low at high pH and the calcite dissolution kinetics are comparably slow compared to atmospheric CO_2 uptake. This concept is contrary to the often supported one that the presence of calcite in the hydrated phase assemblages promotes thaumasite formation [37]. Additionally, in contrast to previous assumptions by some of the authors [38], formation of thaumasite and calcite do not seem to be competing concurring reactions: the samples with the highest carbonation degree were also those with the highest thaumasite content. However, formation of thaumasite and calcite did take place in physically separated areas and no 'joint-precipitation' was observed.

4.2. Presence of gypsum and ettringite

Thaumasite formed only in samples where initial ettringite (5 wt% of total powder mass) had been present. This occurred in finer and coarser ternesite, at low and room temperature. Two of the main differences between the present study and that from Dvorak et al. are the water/solid ratio and the purity of the ternesite considered [21]. Dvorak et al. reported formation of thaumasite during hydration at 5 °C of ternesite, belite, anhydrite and lime, mixed at a water:solid ratio of 3:1 in the absence of ettringite. The samples never hardened as the sampling always took place with a pipette and subsequent drying. In the present study samples did harden and the solids that had been exposed to high RH were directly analyzed. No conclusions were drawn by Dvorak in terms of the effect of the clinker composition; however, the 'suspension state' seems to have a major impact in the formation of thaumasite. This latter could be due to the higher reactive surface available, the shaking energy or the unrestricted crystal growth in suspension. Additionally, the presence of Al impurities cannot be excluded in that study as was the case in the investigation from Skalamprinos et al., where small amounts of ettringite seemed to have formed at very early stages of ternesite hydration [2]. In any case, in accordance with previous studies on the thaumasite form of sulfate attack, the presence of gypsum, or more precisely the supersaturation of gypsum, is required for the formation of thaumasite [19,35].

The potentially supportive effect of ettringite on thaumasite formation could be ascribed to several factors: i) Ettringite provides small amounts of Ca, Al, sulfate, and hydroxide to an aqueous solution it is in equilibrium with. In contrast to calcite and portlandite, ettringite does not only provide some of the ions needed to start the nucleation but, due to their similar crystal structures, ettringite surface can also act as a template and/or nucleation site for thaumasite formation. With available carbonate and silica, nucleation and formation of thaumasite can proceed. For the further growth of thaumasite extra Ca and sulfate, provided by e.g. portlandite and gypsum, are required; ii) Al readily enters octahedral coordination both in aqueous species and upon formation of solid phases. It is possible that a certain amount of aqueous Al, for example released by the dissolution of ettringite, induces co-precipitation of aqueous Si in octahedral coordination. Mixed Al and Si occupancies of octahedral sites are known from solid solutions like for example woodfordite; iii) the carbonation of ettringite, which is usually supported by the same conditions which favor thaumasite formation, can release further sulfate ions supporting continued thaumasite formation; iv) sulfate ions released by equilibrium dissolution or carbonation of ettringite may inhibit the formation of calcite [32], favoring

thaumasite formation instead. Additionally, the conversion of aqueous Ca^{2+} and SO_4^{2-} to gypsum and the uptake of silica via ettringite to thaumasite transformation may stimulate the incongruent dissolution of ternesite and thus the stronger conversion to C-S-H in the presence of ettringite.

4.3. Ternesite hydration activation by Al

As mentioned in the introduction, the presence of aluminium hydroxide or other alumina sources from the hydration of CSA and calcium aluminates have been reported to activate ternesite hydration and to lead to the formation of C-S-H and ettringite [23,24]. However, if ettringite forms before all ternesite had been consumed it may act as a trigger for thaumasite formation, as in the present case. In the studies from [23,24] formation of thaumasite was not reported. This could mean that if ternesite hydration starts before ettringite formation or if carbonation is prevented during hydration, formation of thaumasite may be avoided. However, these studies did not evaluate the systems after months or years and as such the long-term behaviour is not known. On the other hand, most CSA clinkers containing ternesite include high percentages of ye'elimite (and belite) and only small percentages of ternesite. In these systems ettringite is the main hydration product and there are only small amounts of the 'ingredients' needed for thaumasite (coming from ternesite hydration), as opposed to our systems where only seeds of ettringite and large amounts of the components necessary for thaumasite formation were present. Additionally, it is possible that ettringite can 'consume' part of the silica released from ternesite or C-S-H.

Thaumasite formation seems to be promoted by small amounts of Al. At high amounts, above the immiscibility threshold [33,34], C-S-H, straetlingite and eventually (above Al/Si 0.5) ettringite are thermodynamically and probably also kinetically favored. Due to enormous differences between the systems, conclusions from the present study on simplified systems cannot be extrapolated to CSA clinkers containing ternesite. However, it is recommended to address the use of ternesite as alternative clinker with care when formation of ettringite is envisaged within the system.

4.4. Ternesite-based cements durability

Formation of thaumasite itself may not be a problem if not contributing to the disintegration of the C-S-H and thus to the hardened material. In fact, if it forms as a hydration product together with C-S-H and gypsum it may not lead to the physical deterioration of the system. This seems to be the case in most of the samples analyzed here. Physical expansion and disintegration were only observed when exposing ternesite with a very high specific surface area and with ettringite 'seeds' at room T. At this point it is not clear whether the rest of the samples where thaumasite had formed would also present structural disintegration at later stages and what would happen if external sulfate enters the system. As sulfate attack on real structures is known to be a "long-term problem" the respective reaction kinetics have to be assessed before ternesite-based cements can be declared as "sulfate resistant".

5. Conclusions

Synthesized ternesite samples, with BET surface areas of 3.5 and 8.4 m^2/g, were hydrated at 6.5 °C and at room temperature in the presence/absence of ettringite, carbonated ettringite, calcite and portlandite. The following conclusions have been drawn:

- Thaumasite did not form during hydration of pure ternesite, neither at low nor at room temperature, in the time frames considered (1.3 years for the coarser and 4.5 months for the finer ternesite).
- The presence of portlandite and calcite in the ternesite systems did not promote the formation of thaumasite.

- Thaumasite formed, together with gypsum and C-S-H, only in samples where initial ettringite (5 wt% of total powder mass) had been present. This occurred in finer and coarser ternesite, at low and room temperature. The supportive role of ettringite on thaumasite formation is ascribed to the template effect, the provision of ions to start the nucleation, the co-precipitation of aqueous Si in octahedral coordination leading to solid solutions (woodfordite), and the release of sulfate ions during ettringite dissolution and carbonation. Additionally, the uptake of silica in thaumasite may stimulate the dissolution of ternesite and thus the stronger conversion to C-S-H in the presence of ettringite.
- Due to the differences between the simplified systems used in the present study and ternesite-containing CSA clinkers the conclusions drawn here cannot be extrapolated to more complex systems. However, the study should serve as a basis for further investigations related to the durability of ternesite clinkers when ettringite formation is envisaged within the system.

CRediT authorship contribution statement

I. Galan: Conceptualization, Methodology, Investigation, Writing – original draft, Visualization. **F.R. Steindl:** Methodology, Visualization, Writing – review & editing. **C. Grengg:** Investigation, Writing – review & editing. **M. Dietzel:** Validation, Writing – review & editing. **F. Mittermayr:** Validation, Supervision, Visualization, Writing – review & editing.

Declaration of competing interest

The authors declare that they have no known competing financial interests or personal relationships that could have appeared to influence the work reported in this paper.

Data availability

The authors are unable or have chosen not to specify which data has been used.

Acknowledgements

Appendix A

Table A1
Crystallographic information files used for Rietveld refinement.

Phase	ICSD code	Reference
Ternesite	85123	Irran et al., 1997
Beta-belite	81096	Mumme et al., 1996
Gamma-belite	81095	Mumme et al., 1996
Anhydrite	16382	Kirfel et al., 1980
Ettringite	155395	Goetz-Neunhoeffer et al., 2006
Gypsum	151692	De la Torre et al., 2004
Calcite	80869	Maslen et al., 1993
Bassanite	79528	Bezou et al., 1995
Thaumasite	31247	Effenberger et al., 1983
Monohydrocalcite	200820	Effenberger et al., 1981
Aragonite	15194	De Villiers, 1971
Vaterite	15879	Kamhi, 1963

Table A2
Rietveld refinement results of samples containing $T_{8.4}$ after 2 months exposure to 5 °C and room temperature. Note only crystalline phases are considered here. No quantification of the amorphous content in the samples is included.

	T1 5 °C surface	T1-CE 5 °C surface	T1-P 5 °C surface	T1 5 °C bulk	T1-CE 5 °C bulk	T1-P 5 °C bulk	T1 room T bulk	T1-CE room T bulk
Ternesite	8.4	11.6	13.2	33.6	24.4	42.3	36.3	2.5
Gypsum				27.0	18.6	26.7	31.6	25.3
Calcite	37.1	26.7	34.3	24.9	23.6	24.1	30.0	24.9
Monohydrocalcite	48.2	48.2	47.0	11.0	3.3	2.9		
Vaterite	6.3		5.5	3.5		4.0		
Aragonite							2.1	3.5
Ettringite		2.5			2.6			10.0
Thaumasite		11.0			27.5			33.8
wRp	9.4	9.7	10.9	7.8	7.6	7.6	7.1	7.7

Table A3
Unit cell parameters of (a) initial ettringite (added to the anhydrous ternesite), ettringite after the exposure time, and reference values from Goetz-Neunhoeffer [40], and (b) thaumasite formed after the exposure time and reference values from Effenberger et al. [31].

(a)

	Initial ettringite	Ettringite in T1-CE 5 °C	Ettringite in T1-CE room T	Ettringite in T2-E	Ettringite in T2-CE	Ettringite Goetz-Neunhoeffer et al.
a	11.23	11.23	11.24	11.23	11.20	11.23
c/2	10.73	10.70	10.71	10.72	10.59	10.74

(b)

	Thaumasite in T1-CE 5 °C	Thaumasite in T1-CE room T	Thaumasite in T2-E	Thaumasite in T2-CE	Thaumasite Effenberger et al.
a	11.05	11.06	11.06	11.09	11.03
c	10.42	10.43	10.42	10.45	10.40

Table A4
Rietveld refinement results of samples containing $T_{3.5}$ after 1.3 years exposure to room temperature and high RH conditions. Note only crystalline phases are considered here. No quantification of the amorphous content in the samples is included.

	T2	T2-C	T2-CE	T2-E
Ternesite	50.9	53.2	46.1	
Gypsum	27.0	20.9	20.0	27.2
Calcite	16.8	20.1	18.9	32.5
Aragonite	3.7	4.2	3.7	12.0
Beta-belite	0.9	0.5	0.8	0.8
Gamma-belite	0.7	1.1	0.5	0.5
Ettringite			5.0	2.7
Thaumasite			5.0	24.3
wRp	6.3	6.8	6.5	9.0
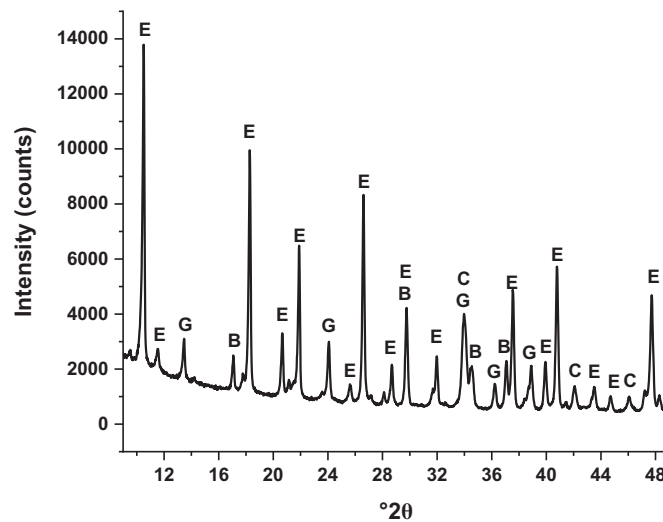
Fig. A1. XRD scan of carbonated ettringite used for the experiments. E: ettringite, G: gypsum, C: calcite, B: bassanite.
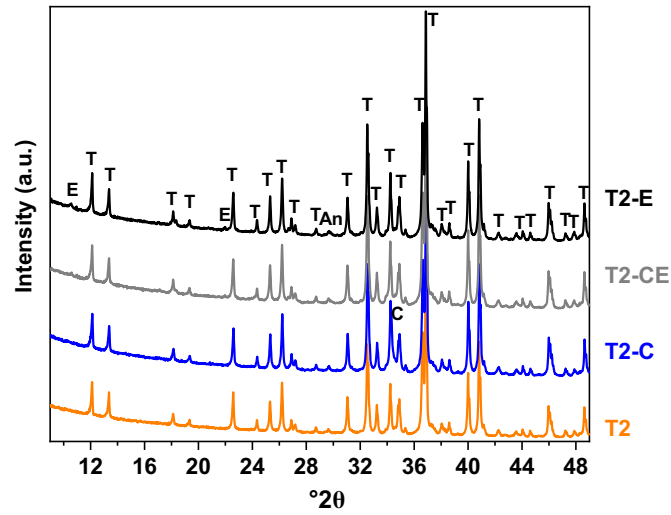
Fig. A2. XRD patterns of anhydrous T2 samples (without additions T2, with calcite T2-C, with carbonated ettringite T2-CE and with ettringite T2-E). T: ternesite, E: ettringite, C: calcite, An: anhydrite.
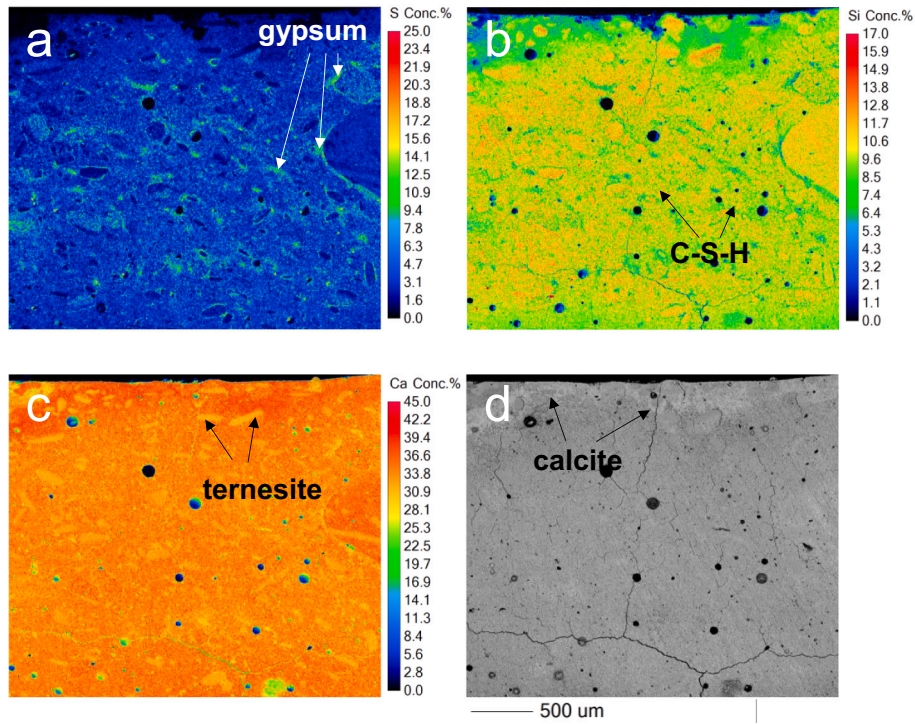

Fig. A3. S, Si and Ca EPMA mappings (a, b, c) and micrograph (d) of T2 after 1.3 years exposure at room temperature.
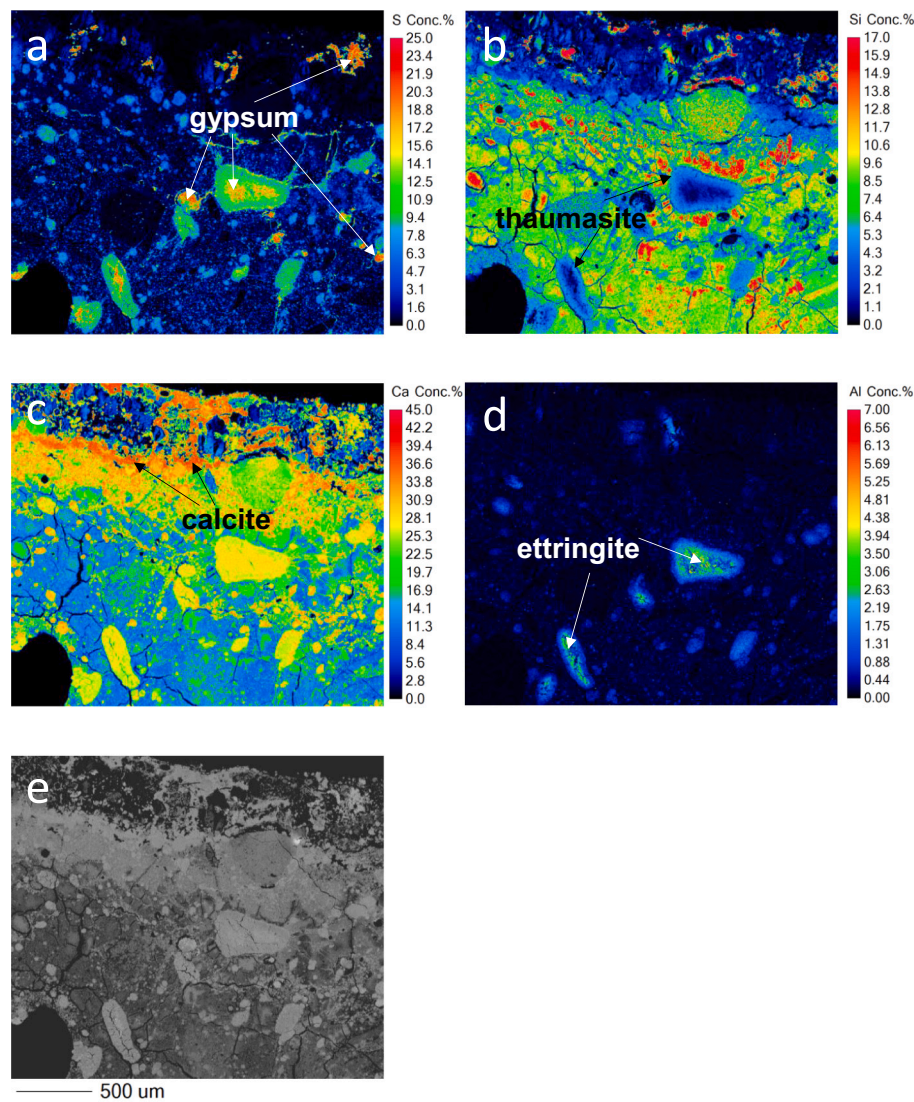
Fig. A4. S, Si, Ca and Al EPMA mappings (a, b, c, d) and micrograph (e) of T2-E after 1.3 years exposure at room temperature.

References

[1] F. Bullerjahn, M. Zajac, M. Ben Haha, CSA raw mix design: effect on clinker formation and reactivity, Mater. Struct. Constr. 48 (2015) 3895–3911, https://doi.org/10.1617/s11527-014-0451-z.

[2] S. Skalamprinos, G. Jen, I. Galan, M. Whittaker, A. Elhoweris, F.P. Glasser, The synthesis and hydration of ternesite, Ca5(SiO4)2SO4, Cem. Concr. Res. 113 (2018) 27–40.

[3] Y. Shen, J. Qian, Y. Huang, D. Yang, Synthesis of belite sulfoaluminate-ternesite cements with phosphogypsum, Cem. Concr. Compos. 63 (2015) 67–75, https://doi.org/10.1016/j.cemconcomp.2015.09.003.

[4] I. Galan, A. Elhoweris, T. Hanein, M.N. Bannerman, F.P. Glasser, Advances in clinkering technology of calcium sulfoaluminate cement, Adv. Cem. Res. 29 (2017), https://doi.org/10.1680/jadcr.17.00028.

[5] T. Hanein, I. Galan, F.P. Glasser, S. Skalamprinos, A. Elhoweris, M.S. Imbabi, M. N. Bannerman, Stability of ternesite and the production at scale of ternesite-based clinkers, Cem. Concr. Res. 98 (2017), https://doi.org/10.1016/j.cemconres.2017.04.010.

[6] N.J. Crammond, The thaumasite form of sulfate attack in the UK, Cem. Concr. Compos. 25 (2003), https://doi.org/10.1016/S0958-9465(03)00106-9.

[7] J. Bensted, Thaumasite—direct, woodfordite and other possible formation routes, Cem. Concr. Compos. 25 (2003) 873–877, https://doi.org/10.1016/S0958-9465(03)00115-X.

[8] K. Sotiriadis, P. Mácová, A.S. Mazur, A. Viani, P.M. Tolstoy, S. Tsivilis, Long-term thaumasite sulfate attack on Portland-limestone cement concrete: a multi-technique analytical approach for assessing phase assemblage, Cem. Concr. Res. 130 (2020), https://doi.org/10.1016/j.cemconres.2020.105995.

[9] S. Köhler, D. Heinz, L. Urbonas, Effect of ettringite on thaumasite formation, Cem. Concr. Res. 36 (2006), https://doi.org/10.1016/j.cemconres.2005.11.006.

[10] P. Pipilikaki, D. Papageorgiou, C. Teas, E. Chaniotakis, M. Katsioti, The effect of temperature on thaumasite formation, Cem. Concr. Compos. 30 (2008) 964–969, https://doi.org/10.1016/j.cemconcomp.2008.09.004.

[11] G. Kakali, S. Tsivilis, A. Skaropoulou, J.H. Sharp, R.N. Swamy, Parameters affecting thaumasite formation in limestone cement mortar, in, Cem. Concr. Compos. (2003) 977–981, https://doi.org/10.1016/S0958-9465(03)00119-7.

[12] S. Martinez-Ramirez, M.T. Blanco-Varela, J. Rapazote, Thaumasite formation in sugary solutions: effect of temperature and sucrose concentration, Constr. Build. Mater. 25 (2011) 21–29, https://doi.org/10.1016/j.conbuildmat.2010.06.061.

[13] H. Justnes, Thaumasite formed by sulfate attack on mortar with limestone filler, Cem. Concr. Compos. 25 (2003), https://doi.org/10.1016/S0958-9465(03)00120-3.

[14] S. Tsivilis, K. Sotiriadis, A. Skaropoulou, Thaumasite form of sulfate attack (TSA) in limestone cement pastes, J. Eur. Ceram. Soc. 27 (2007) 1711–1714, https://doi.org/10.1016/j.jeurceramsoc.2006.05.048.

[15] G. Collett, N.J. Crammond, R.N. Swamy, J.H. Sharp, The role of carbon dioxide in the formation of thaumasite, Cem. Concr. Res. 34 (2004), https://doi.org/10.1016/j.cemconres.2004.02.024.

[16] M. Dietzel, E. Usdowski, J. Hoefs, Chemical and 13C/12C-and 18O/16O-isotope evolution of alkaline drainage waters and the precipitation of calcite, Appl. Geochem. 7 (1992) 177–184, https://doi.org/10.1016/0883-2927(92)90035-2.

[17] M.T. Blanco-Varela, P.M. Carmona-Quiroga, I.F. Sáez Del Bosque, S. Martínez-Ramírez, Role of organic admixtures on thaumasite precipitation, Cem. Concr. Res. 42 (2012) 994–1000, https://doi.org/10.1016/j.cemconres.2012.03.020.

[18] J. Aguilera, M.T.B. Varela, T. Vázquez, Procedure of synthesis of thaumasite, Cem. Concr. Res. 31 (2001) 1163–1168, https://doi.org/10.1016/S0008-8846(01)00536-1.

[19] F. Mittermayr, A. Baldermann, C. Kurta, T. Rinder, D. Klammer, A. Leis, J. Tritthart, M. Dietzel, Evaporation — a key mechanism for the thaumasite form of sulfate attack, Cem. Concr. Res. 49 (2013) 55–64, https://doi.org/10.1016/j.cemconres.2013.03.003.

[20] F. Mittermayr, C. Bauer, D. Klammer, M.E. Böttcher, A. Leis, P. Escher, M. Dietzel, Concrete under sulphate attack: an isotope study on sulphur sources, Isot. Environ. Health Stud. 48 (2012) 105–117, https://doi.org/10.1080/10256016.2012.641964.

[21] K. Dvorak, D. Vsiansky, D. Gazdic, M. Fridrichova, D. Vaiciukyniene, Thaumasite formation by hydration of sulphosilicate clinker, Mater. Today Commun. 25 (2020), https://doi.org/10.1016/j.mtcomm.2020.101449.

[22] K. Dvorak, M. Fridrichova, D. Gazdic, Study of formation of thaumasite on hydration of ternesite clinker, in: 15th Int. Congr. Chem. Cem., Prague, 2019.

[23] M. Ben Haha, F. Bullerjahn, M. Zajac, On the reactivity of ternesite, in: Proc. 14th Int. Congr. Chem. Cem, 2015.

[24] M. Montes, E. Pato, P.M. Carmona-Quiroga, M.T. Blanco-Varela, Can calcium aluminates activate ternesite hydration? Cem. Concr. Res. 103 (2018) 204–215, https://doi.org/10.1016/j.cemconres.2017.10.017.

[25] P.M. Carmona-Quiroga, M. Montes, E. Pato, A. Fernández-Jiménez, M.T. Blanco-Varela, Study on the activation of ternesite in CaO·Al2O3 and 12CaO·7Al2O3 blends with gypsum for the development of low-CO2 binders, J. Clean. Prod. 291 (2021), https://doi.org/10.1016/j.jclepro.2020.125726.

[26] Y. Shen, X. Chen, W. Zhang, X. Li, Effect of ternesite on the hydration and properties of calcium sulfoaluminate cement, J. Therm. Anal. Calorim. 136 (2019) 687–695, https://doi.org/10.1007/s10973-018-7685-x.

[27] Y. Shen, P. Wang, X. Chen, W. Zhang, J. Qian, Synthesis, characterisation and hydration of ternesite, Constr. Build. Mater. 270 (2021), https://doi.org/10.1016/j.conbuildmat.2020.121392.

[28] M. Balonis, F.P. Glasser, The density of cement phases, Cem. Concr. Res. 39 (2009) 733–739, https://doi.org/10.1016/j.cemconres.2009.06.005.

[29] P. Lanari, A. Vho, T. Bovay, L. Airaghi, S. Centrella, Quantitative compositional mapping of mineral phases by electron probe micro-analyser, Geol. Soc. Spec. Publ. 478 (2019) 39–63, https://doi.org/10.1144/SP478.4.

[30] R.A. Edge, H.F.W. Taylor, Crystal structure of thaumasite, a mineral containing [Si (OH)6]2- groups, Nature 224 (1969) 363–364, https://doi.org/10.1038/224363a0.

[31] H. Effenberger, A. Kirfel, G. Will, E. Zobetz, A further refinement of the crystal structure of thaumasite, Ca3Si(OH)6CO3SO4.12H2O, in: Neues Jahrb. Fur Mineral. Monatshefte, 1983, pp. 60–68. https://www.scopus.com/inward/record.uri?eid=2-s2.0-0020542017&partnerID=40&md5=5a8473a8186e8a5fb2b8fd94c9f6c6a7.

[32] K.E. Goetschl, B. Purgstaller, M. Dietzel, V. Mavromatis, Effect of sulfate on magnesium incorporation in low-magnesium calcite, Geochim. Cosmochim. Acta 265 (2019) 505–519, https://doi.org/10.1016/j.gca.2019.07.024.

[33] S.J. Barnett, D.E. Macphee, N.J. Crammond, Extent of immiscibility in the ettringite-thaumasite system, Cem. Concr. Compos. 25 (2003) 851–855, https://doi.org/10.1016/S0958-9465(03)00116-1.

[34] S.J. Barnett, D.E. Macphee, E.E. Lachowski, N.J. Crammond, XRD, EDX and IR analysis of solid solutions between thaumasite and ettringite, Cem. Concr. Res. 32 (2002) 719–730, https://doi.org/10.1016/S0008-8846(01)00750-5.

[35] F. Mittermayr, A. Baldermann, C. Baldermann, G.H. Grathoff, D. Klammer, S. J. Köhler, A. Leis, L.N. Warr, M. Dietzel, Environmental controls and reaction pathways of coupled de-dolomitization and thaumasite formation, Cem. Concr. Res. 95 (2017), https://doi.org/10.1016/j.cemconres.2017.02.011.

[36] F. Bellmann, J. Stark, The role of calcium hydroxide in the formation of thaumasite, Cem. Concr. Res. 38 (2008) 1154–1161, https://doi.org/10.1016/j.cemconres.2008.04.005.

[37] T. Schmidt, B. Lothenbach, M. Romer, K. Scrivener, D. Rentsch, R. Figi, A thermodynamic and experimental study of the conditions of thaumasite formation, Cem. Concr. Res. 38 (2008), https://doi.org/10.1016/j.cemconres.2007.11.003.

[38] F. Mittermayr, M. Rezvani, A. Baldermann, S. Hainer, P. Breitenbücher, J. Juhart, C. Graubner, T. Proske, Sulfate resistance of cement-reduced eco-friendly concretes, Cem. Concr. Compos. 55 (2015) 364–373, https://doi.org/10.1016/j.cemconcomp.2014.09.020.

[39] W. Lukas, Betonzerstörung durch SO3-angriff unter bildung von thaumasit und woodfordit, Cem. Concr. Res. 5 (1975) 503–517, https://doi.org/10.1016/0008-8846(75)90025-3.

[40] F. Goetz-Neunhoeffer, J. Neubauer, Refined ettringite (Ca6 Al2 (SO4) 3 (OH)12 ·26 H2O) structure for quantitative X-ray diffraction analysis, Powder Diffract. 21 (2006) 4–11, https://doi.org/10.1154/1.2146207.